Wave-Particle Dynamics of Wave Breaking in the Self-Excited Dust Acoustic Wave

Lee-Wen Teng, Mei-Chu Chang, Yu-Ping Tseng, and Lin I

Department of Physics and Center for Complex Systems, National Central University, Jhongli, Taiwan 32001, Republic of China

(Received 27 July 2009; revised manuscript received 1 November 2009; published 11 December 2009)

The wave-particle microdynamics in the breaking of the self-excited dust acoustic wave growing in a dusty plasma liquid is investigated through directly tracking dust micromotion. It is found that the nonlinear wave growth and steepening stop as the mean oscillating amplitude of dust displacement reaches about $1/k$ (k is the wave number), where the vertical neighboring dust trajectories start to crossover and the resonant wave heating with uncertain crest trapping onsets. The dephased dust oscillations cause the abrupt dropping and broadening of the wave crest after breaking, accompanied by the transition from the liquid phase with coherent dust oscillation to the gas phase with chaotic dust oscillation. Corkscrew-shaped phase-space distributions measured at the fixed phases of the wave oscillation cycle clearly indicate how dusts move in and constitute the evolving waveform through dust-wave interaction.

DOI: 10.1103/PhysRevLett.103.245005 PACS numbers: 52.27.Lw, 05.45.−a, 52.25.Gj, 52.35.Fp

Associated with the sudden drop of wave amplitude, the breaking of a growing wave after reaching certain critical amplitude is a fundamental nonlinear wave phenomenon. It occurs not only in the well-known example of the wave driven by the strong wind on the water surface, but also in longitudinal density waves [1–11]. In plasma waves, wave breaking have been mainly studied on the longitudinal electron plasma wave [2–11]. High speed electron acceleration and heating were demonstrated at and beyond electron plasma wave breaking in laser wake field accelerators [7,8,12] and pulsed laser-solid interaction [10,11].

As the wave amplitude grows, the waveform becomes nonsinusoidal and steepens. The early theoretical work for the electron plasma wave in the *cold plasma* neglecting thermal effect pointed out that nonlinearity leads to wave breaking at the critical particle oscillating amplitude $\sim 1/k$ (k is the wave number), associated with fine scale mixing [2]. Microscopically, the waveform evolution is self-consistently determined by the constituting particles whose oscillatory motions are in turn strongly affected by the wave field and local heterogeneity, especially when the wave amplitude is large [13]. Wave breaking is certainly a complicated nonlinear kinetic issue, in which the phase-space dynamics plays an important role. The previous theoretical, numerical and experimental studies on the electron plasma wave indicated the strong wave-particle interaction in the growing wave can heat up particles, with some particles reaching wave phase velocity [3–8,11]. The disordered particle motion and the wave energy consumption, which oppose the growing wave reaching singularity, have been proposed to explain wave breaking [3–8,11]. Nevertheless, no experimental studies have been conducted at the discrete microscopic level through directly visualizing particle motion to illustrate the generic wave-particle dynamics of the wave breaking for the longitudinal density waves, especially in the phase space at the fixed phase ϕ of the wave oscillation cycle.

The dust acoustic wave (DAW), propagating through the interplay of dust inertia, the screened electric field and plasma pressure, is a fundamental wave in the dusty plasma composed of negatively charged (about 10^4 electrons per dust particle) micrometer dust particles suspended in the low pressure gaseous plasma background [14–19]. It can be self-excited and grow in the laboratory discharge system by the free energy source such as ion streaming [16]. The capability of directly tracking individual dust motion makes the DAW a paradigm to understand the generic wave-particle microdynamics of the longitudinal density waves at the discrete kinetic level [18,19], beyond the conventional macroscopic studies.

In this Letter, using the DAW self-excited by the downward ion flow in a 3D rf *dusty plasma liquid* as an example, we report the first experimental study on the Eulerian and Lagrangian wave-particle phase-space dynamics for wave breaking, through correlating individual dust motion and density waveform evolution. The critical averaged dust oscillating amplitude for wave breaking is identified. It is found that, before breaking, the wave exponentially grows and steepens as the amplitudes of coherently oscillating dusts grow. The associated increasing wave crest compression induces liquid-gas transition to the state with chaotic dust oscillation after the onsets of dust trajectories crossing and the uncertain resonant dust trapping. The induced dephased chaotic dust oscillation is the key for breaking. The wave-particle interaction induces corkscrew-shaped phase-space distributions at fixed phases ϕ of the wave oscillation cycle. A micropicture is constructed to illustrate how dusts move in, interact with, and constitute the evolving waveform.

The experiment is conducted in a cylindrical symmetric rf dusty plasma system similar to our previous experiment [19]. As shown in Fig. 1(a), a hollow coaxial cylindrical trap with 3-cm inner diameter and 18 mm height is put on the bottom electrode to confine the dusty plasma with

polystyrene particles (5 μm in diameter). The weakly ionized glow discharge ($n_e \sim 10^9$ cm^{-3}) is generated in Ar gas at 200 mTorr using a 14-MHz rf power system. At low rf power, dusts are in the cold liquid state. The interdust distance is about 0.3 mm. The dust mass and the dust charge are 6.9×10^{-11} g/dust and about $5000e$/dust, respectively. The Debye length λ_D is about 100 μm. The downward ion flow toward the negatively self-biased bottom provides a free energy source to drive the DAW. An expanded thin vertical laser sheet through the trap is used for illuminating the dust motion in the vertical plane. The video images by a CCD camera at 500 Hz frame rate are digitally processed. The statistical measurements are obtained from about 400 dusts and 45 oscillating cycles.

The downward propagating DAW with oscillation frequency $f_0 = 22.5$ Hz can be self-excited by the downward ion flow while increasing rf power to 2.6 W. Figure 1(b) and 1(c) show the typical sequential snapshots of dust images and the spatiotemporal evolution of the normalized dust density $n_d(z, t) = I_d(z, t)/\langle I_d(z)\rangle$, where $\langle I_d(z)\rangle$ is the time average of the scattered laser light intensity $I_d(z)$, coarse grained over the rectangle 0.1 mm in height and 2.5 mm in width at height z. The waveform has small amplitude n_0 in the upper region. With decreasing z, the waveform steepens [Fig. 1(c)], associated with the exponential growth of n_0 with exponent (spatial growth rate) = 3 mm^{-1} [Fig. 2(a)]. The following rapid decay and leveling off signify the wave breaking, regardless of the slow smooth rise and saturation of δz [Fig. 2(c)]. δz is the averaged oscillation amplitude of single dust motion measured from the rising part of the trajectories in the z-t space. We set $z = 0$ for the breaking point, where the crest has the narrowest width and the maximum height [also see the narrow bright strip in Fig. 1(b)]. The spatial variations of the temporal waveform harmonics in Fig. 2(b) show the similar trend, with more serious dropping for the higher order harmonics after breaking. Namely, the steepened waveform deviates most from the sinusoidal waveform at the breaking point. Note that wave breaking occurs at $\delta z \sim 1/k$ (k is the wave number) [Fig. 2(c)], which is about the same predicted scale for the breaking of the electron density wave in the cold plasma [2].

To characterize the degree of disordering of individual dust motion in the evolving wave, we measure the spatial variation of Lyapunov exponent λ_L by tracking dust trajectories [Fig. 2(d), also see the dust trajectories in Fig. 3(a)]. λ_L is obtained from the exponent of the averaged temporal divergent rate of the distance $\delta X_z(t + \Delta t)$ between the states of a dust pair with initial vertical position at z in the (z, v_z) phase space and the small initial distance $\delta X_z(t)$ [i.e., $\delta X_z(t + \Delta t) = \delta X_z(t) \exp(\lambda_L \Delta t)$], where $\Delta t = 10$ ms [20]. λ_L shows a fast rise from nearly zero before wave breaking and saturate at about $2.3 f_0$ after breaking. It indicates the transition from the ordered coherent oscillation in the liquid state to the gas state with

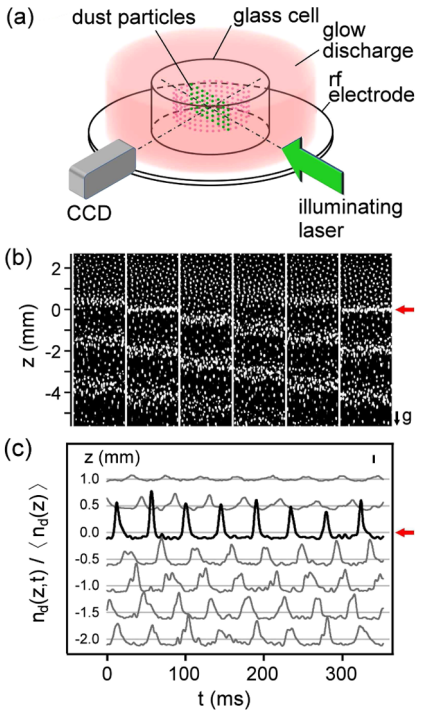

FIG. 1 (color online). (a) The sketch showing the experimental system. (b) The sequential snap shots of the dust images with 1 ms exposure time and 10 ms interval. (c) The normalized dust density profiles $n_d(z, t)$ at a few typical heights. The gray horizontal lines in (c) correspond to $n_d = 1$. The vertical bar at the upper right corner of (c) indicates the scale of $n_d = 1$. The breaking occurs at $z = 0$ mm where the crest height (width) reaches the maximum (minimum). The arrows in (b) and (c) indicate the positions for wave breaking.

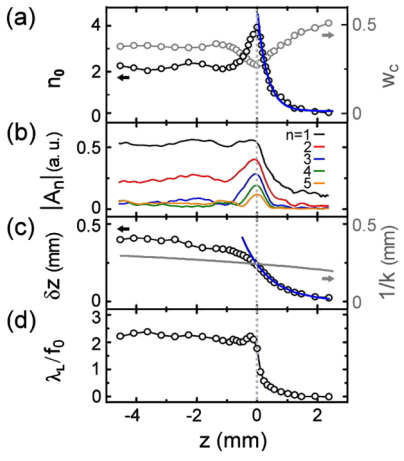

FIG. 2 (color online). (a) The spatial variations of the normalized wave amplitude n_0 and the crest width w_c (measured at $n_d = 1$ and normalized by the wave period $\tau = 1/f_0$). The upward bending solid curve shows the exponential growth fits with spatial growth rate = 3.0 mm^{-1}. (b) The spatial variations of the amplitudes, A_n of the fundamental ($n = 1$), and harmonics ($n = 2$ to 5) of the normalized density waveform. (c) and (d) The averaged dust oscillating amplitude δz, the inverse of wave number $1/k$, and the Lyapunov exponent λ_L normalized by the wave frequency f_0, respectively.

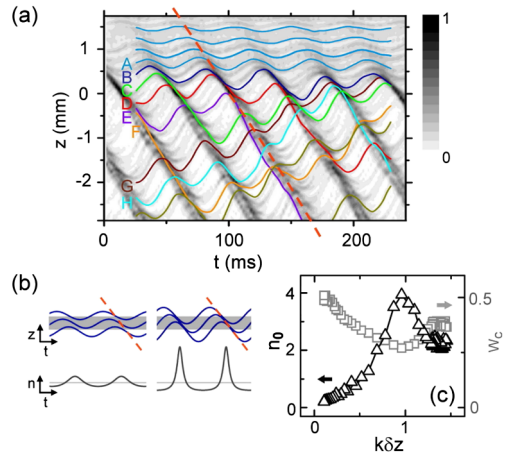

FIG. 3 (color online). (a) Temporal evolutions of dust vertical positions using the plot of coarse-grained scattered light intensity as a reference background to show how dusts move in the density wave. The dark regions correspond to crest regions. (b) The sketch showing how the density waveforms (lower row, obtained directly from the inverse of the local interdust distance in the gray band) steepen with the increasing amplitude of the oscillating trajectories of the neighboring dust particles (curves in the upper row). The tilted dashed lines in (a) and (b) depict the trajectories of density crests. (c) The plot showing the nonlinear dependences of n_0 and w_c on $k\delta z$.

chaotic oscillation at wave breaking. This can be further evidenced by dust trajectory plots in Fig. 3(a). The onset of chaotic dust motion is associated with the onset of trajectory crossing of nearby dust pairs around breaking ($z = 0$ mm).

Now let us construct a picture to explain the micro-origin of wave breaking, using the dust trajectory plots on top of the contour plot of the dust density waveform (the dark region corresponds to the wave crest) in the z-t space [Fig. 3(a)], to connect Lagrangian and Eulerian views. Excited by the downward ion wind, the wave starts growing from the upper cold liquid state region, in which dusts exhibit small amplitude *coherent* oscillations [see the motions of dusts above dust A in Fig. 3(a)]. For an ideal 1D system as shown in the sketches of Fig. 3(b), the local dust density is inversely proportional to the distance Δz between the two local vertical neighboring particles. Therefore, the rising and the descending regions of the dust trajectory correspond to the trough and the crest in the density waveform, respectively [Figs. 3(a) and 3(b)]. The crest height $n_0 + 1$ is inversely proportional to $\Delta z_{\min}$, the minimum Δz in a dust oscillation cycle. The phase lag $\Delta\psi$ between the two oscillating neighboring dusts i and j with equilibrium vertical separation $\Delta z_{0,ij}$ follows $\Delta\psi = k\Delta z_{0,ij}$. Increasing δz and increasing k can make the two neighboring trajectories closer in the trajectory descending region. It nonlinearly steepens the waveform, increases the crest height, and decreases the crest width [Figs. 3(b) and 3(c)]. A simple mathematical derivation shows that, for the two neighboring dusts exhibiting sinusoidal oscillations, their trajectories start to touch each other (i.e., $\Delta z_{\min} = 0$), when $k\delta z$ reaches 1. In reality, the associated density singularity at $k\delta z = 1$ is opposed by the strong Coulomb repulsion at the small interdust distance. Namely, the strong compression and local heterogeneity make dust trajectories in the z-t space deviate from sinusoidal oscillation and exhibit uncertain rebound or crossover (through the extra transverse motion) after dust-dust collision [e.g., see the trajectories of dust in the crests regions for $z = \pm 0.2$ mm in Fig. 3(a)] in the crest region. The uncertainty effect can propagate backward to $z = 1$ mm due to the finite dust oscillation amplitude and Coulomb interaction. The downward dust after crossing can be temporally trapped around the crest with uncertain trapping time [e.g., see the downward trajectories of dust A to F in Fig. 3(a)] [19]. It onsets the transition from the cold liquid with coherent dust oscillation to the gas state with disordered dust oscillation at breaking. The dephased dust oscillation, which less coherently constitutes the wave, is the key micro-origin for breaking with n_0 dropping and w_c increasing, until reaching the steady state with the further slow increase of δz. Note that the dust density oscillation in the DAW still keeps long time correlation after breaking regardless of the chaotic individual dust oscillation [Fig. 1(c)].

How does the density waveform in turn affect the dust dynamics in the z-v_z phase space before and after the breaking through wave-particle interaction? Figure 4(a) to 4(c) depict the corkscrew-shaped distributions (each black dot represents a single dust state) of about 400 dusts in the z-v_z space measured at three different phases of the density wave oscillation cycle. The gray curves and the dashed lines depict the corresponding waveform $n_d(z)$ and the crest velocity $v_c(z)$, respectively. We set phase $\phi = 0$, as one of the crests reaches $z = 0$ mm, where the crest height reaches the maximum. Note that the left edge of the

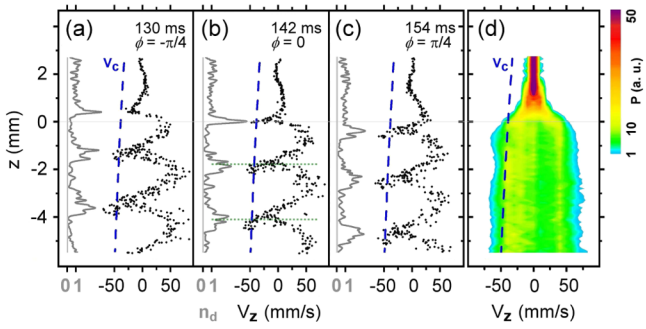

FIG. 4 (color online). (a) to (c) The phase-space distributions of dust micromotion at different phases ϕ of the wave oscillating cycle. $\phi = 0$ is defined as one of the crests reaches $z = 0$ mm. Each dot represents the state of one dust. The gray curve in each panel depicts the corresponding spatial density waveform $n_d(z)$. (d) The contour plot of the averaged dust velocity distribution $P(v_z, z)$ over 45 oscillating cycles. The dashed lines in (a) to (d) depict the v_c spatial variation. The wave breaking is associated with the onset of resonant heating of dusts by the wave.

distribution starts to cross the dashed line at $\phi = 0$. Dusts are negatively charged and repel each other through screened Coulomb interaction. Namely, in the wave, the dust moves in a traveling washboard type electric potential energy field oscillating in phase with n_d oscillation [13,19]. Before breaking ($z > 0$ mm), the dust velocity in the wave frame, $v_z' = v_z - v_c$, always remaining positive evidences that the downward traveling small potential crest cannot trap the dust. It only causes coherent small amplitude dust oscillation in the *cold liquid* state with small v_z spread at fixed z and fixed ϕ. The upward moving dusts are pushed downward by the wave crest front, then quickly enter and leave the crest rear, and move upward again [e.g., dusts above dust A in Fig. 3(a)].

Approaching the breaking point, the stronger field with the growing crest makes mean v_z' smaller at the crest position. It in turn sustains the growing n_0 according to the continuity equation. Then the crossing of v_z' over zero (i.e., $v_z = v_c$) at $\phi = 0$ triggers the breaking. It indicates the onset of *resonant wave trapping*. After breaking, the crest front is constituted by dusts with small positive and negative v_z' [e.g., see the black dots right below the horizontal dotted lines in Fig. 4(b)]. However, in the crest rear, v_z' is small but positive. The upward moving dusts from the wave trough (those in the right arms of the distribution plots) lose their kinetic energies in the crest moving frame, while entering the crest front. They become part of the crest and move downward ($v_z < 0$). They eventually enter the crest rear, leave the crest ($v_z' > 0$) and move upward ($v_z > 0$) to the right arm again, after been pushed upward by other upward moving dusts entering the crest later. The uncertain dwell time around the crest due to the low kinetic energy (in the crest frame) and the uncertain local heterogeneity lead to the chaotic dust oscillation with positive λ_L. The induced large v_z spread at fixed z and ϕ after breaking manifests *wave heating* and dephased dust oscillation, which less constructively sustains the crest. Those dusts with $v_z' \sim 0$ are resonantly trapped by the crest and can travel downward with uncertain long distance, as illustrated in the example of the long downward trajectories of dusts C, D, E, and H in Fig. 3(a). The averaged velocity histogram $P(v_z, z)$ over 45 oscillating cycles has a bottle shape [Fig. 4(d)]. Its left edge reaching v_c at $z = 0$ evidences again the onset of resonant trapping at breaking. Only a small fraction of dusts move faster than the crest speed.

In conclusion, we have experimentally explored the wave-particle dynamics and the micro-origin of wave breaking in the self-excited DAW growing from the liquid state. The important findings are listed as follows: (i) The small amplitude density wave cannot trap dusts. All the dusts remain in the cold liquid state and oscillate coherently with small δz. (ii) The growing wave exponentially steepens, as the minimum distance between the neighboring dust trajectories nonlinearly decreases with the increasing δz. Eventually, the strong compression and the local heterogeneity in the large amplitude crest lead to the uncertain crossover of the neighboring trajectories at $\delta z \sim 1/k$, accompanied by the rapid transition to the disordered gas state with positive λ_L. The onset of dephased dust oscillations with increasing δz, which less coherently constitute the wave is the major cause for breaking with n_0 dropping and w_c increasing. (iii) From the wave-particle interaction view, the onset of uncertain resonant crest trapping after neighboring trajectories crossing triggers the breaking and induces the disordered dust oscillation. The upward moving dusts can be pushed downward and temporarily trapped in the downward moving crest front, and move upward again after leaving the crest rear. It causes the corkscrew-shaped distributions, with larger v_z spread which manifests strong wave heating after breaking, in the phase space at fixed ϕ.

The authors would like to thank Professor C. S. Liu for pointing out the importance of the wave breaking issue. This work is supported by the National Science Council of the Republic of China under Contract No. NSC96-2112-M008-012-MY3.

[1] R. J. Dean and R. A. Dalrymple, *Coastal Processes with Engineering Applications* (Cambridge University Press, Cambridge, England, 2002).
[2] J. A. Dawson, Phys. Rev. **113**, 383 (1959).
[3] T. P. Coffey, Phys. Fluids **14**, 1402 (1971).
[4] M. N. Rosenbluth and C. S. Liu, Phys. Rev. Lett. **29**, 701 (1972).
[5] T. Katsouleas and W. B. Mori, Phys. Rev. Lett. **61**, 90 (1988).
[6] B. S. Bauer, A. Y. Wong, V. K. Decyk, and G. Rosenthal, Phys. Rev. Lett. **68**, 3706 (1992).
[7] S. V. Bulanov, N. Naumova, F. Pegoraro, and J. Sakai, Phys. Rev. E **58**, R5257 (1998).
[8] A. Modena *et al.*, Nature (London) **377**, 606 (1995).
[9] T. Hosokai *et al.*, Phys. Rev. Lett. **97**, 075004 (2006).
[10] Th. Schlegel *et al.*, Phys. Rev. E **60**, 2209 (1999).
[11] A. S. Sandhu, G. R. Kumar, S. Sengupta, A. Das, and P. K. Kaw, Phys. Rev. Lett. **95**, 025005 (2005).
[12] A. Pukhov and J. Meyer-ter-Vehn, Appl. Phys. B **74**, 355 (2002).
[13] E.g., F. F. Chen, *Introduction to Plasma Physics* (Plenum Press, New York, 1974), Chap. 7.
[14] N. N. Rao, P. K. Shukla, and M. Y. Yu, Planet. Space Sci. **38**, 543 (1990); P. K. Shukla, Phys. Scr. **45**, 504 (1992).
[15] A. Barkan, R. L. Merlino, and N. D'Angelo, Phys. Plasmas **2**, 3563 (1995).
[16] P. Kaw and R. Singh, Phys. Rev. Lett. **79**, 423 (1997); A. A. Mamun and P. K. Shukla, Phys. Plasmas **7**, 4412 (2000).
[17] A. Piel *et al.*, Phys. Rev. Lett. **97**, 205009 (2006).
[18] M. Schwabe *et al.*, Phys. Rev. Lett. **99**, 095002 (2007); C. Y. Tsai *et al.*, Phys. Plasmas **16**, 063702 (2009).
[19] C. T. Liao *et al.*, Phys. Rev. Lett. **100**, 185004 (2008).
[20] S. H. Strogatz, *Nonlinear Dynamics and Chaos* (Addison-Wesley, Reading, 1994), Chap. 9.